

Modelling of dew point operating conditions in a rotary regenerative air heater

Warren Brandt^{1*}, Walter Schmitz², Thomas John Sheer², and Mike Lander³

¹Eskom Power Plant Engineering Institute; Boiler Combustion; School of Mechanical, Industrial and Aeronautical Engineering, Private Bag 3, WITS 2050 Johannesburg, South Africa

²School of Mechanical, Industrial and Aeronautical Engineering, University of the Witwatersrand, Private Bag 3, WITS 2050 Johannesburg, South Africa

³Eskom; Research Testing and Development; PEI Draught Plant Specialist, Johannesburg, South Africa

Abstract: Dew point related fouling of regenerative rotary air heaters contributes to efficiency reduction of coal-fired boilers. This fouling commonly causes high pressure differences over the air heater steel matrix, along with elevated leakage rates, resulting in increased loading of draught group fans. These increases also conduce to excessive erosion rates, introducing premature failure of element packs and draught group components. The research problem aimed to develop, and validate, a modelling tool to predict the onset of dew point related fouling for regenerative rotary air heaters (VBA RAH model). A modelling tool equip system engineers with the knowledge to enhance operating conditions and maintenance strategies, to prevent the onset of dew point related fouling. The results yielded that the cold end of the air heater packs experience sulphuric acid dew point related fouling for at 670MW(90% MCR), at 544MW(80% MCR) and at 468MW(68% MCR) of the exposure time to the flue gas stream. Different operating and design change configurations were simulated to find potential solutions to minimize dew point related fouling and improving boiler efficiency. The tool provides a platform for identifying methods to reduce maintenance costs and production losses, which will contribute to improved and sustainable operating of coal fired power generation plants.

1 Introduction

In coal fired power generating plants, air heaters are used to transfer the thermal energy in the flue gas to the combustion air entering the boiler, as stated in Figure 1. A regenerative air heater comprises a steel matrix of stacked element plates. An induced draught fan extracts hot flue gas from the furnace which passes through the steel matrix, transferring heat from the flue gas to the element plates. A forced draught fan blows cold air through the hot element plates, which heat the combustion air to improve the boiler performance. If the thermal performance of an air heater deteriorates, the boiler performance reduce accordingly. Therefore, air heaters are usually one of the major contributors to reduction in energy

* Warren Brandt: brandtwa@eskom.co.za

availability from coal fired power generating plants. A common problem for regenerative air heaters is dew-point related cold end fouling, which leads to insufficient heat transfer.

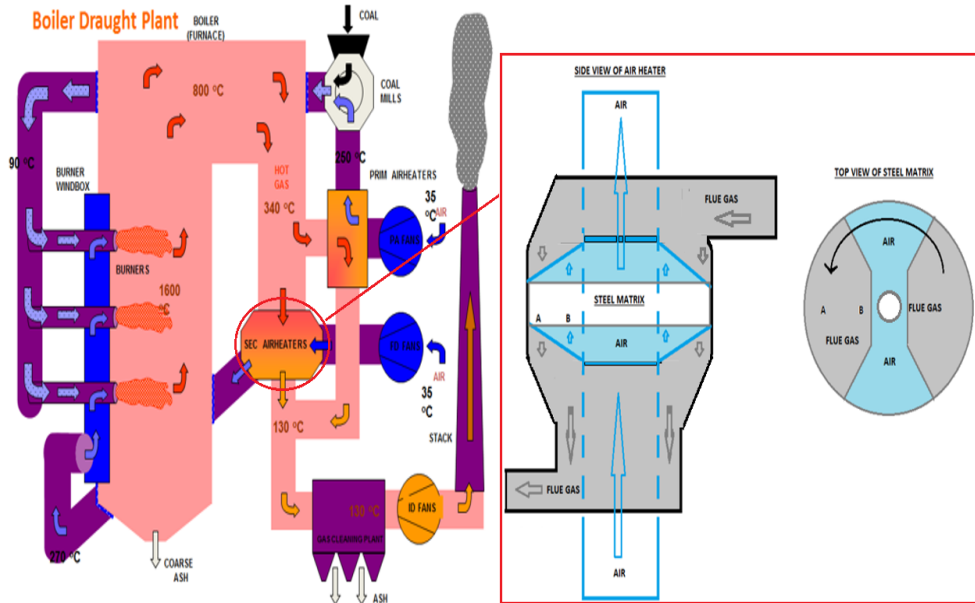


Fig. 1. Boiler process flow schematic.

The following operating conditions are indicators of regenerative air heater dew-point related fouling [1]:

- Occurrences of high pressure differences across the air heater steel matrix, resulting in high FD (Forced Draught) and ID (Induced Draught) fan loading (FD and ID fans operating at maximum capacity).
- Increased fly ash erosion rates occur on localised areas of the air heater steel matrix air heater hoods, dampers and ducts up to the Electrostatic Precipitators (ESP) or Fabric Filter Plant (FFP) inlet-casing.
- Accelerated wear and premature failure of element packs on the steel matrix periphery.
- Exaggerated dust emission levels occur because of augmented volumes of flue gas extracted from the furnace. The fouled element packs restrict flow, which then requires the radial vanes to open more from the FD and ID fans. This introduces increased volumetric flow, which also elevates the flue gas velocity to a point that the ESP becomes less efficient. Dust handling plants with filter bags experience excessive erosion, which reduces the life expectancy of the filter bags. The particle count for the emissions will increase, resulting in additional load losses. Second, the increased velocities also cause higher erosion rates in the air heaters and flue gas ducting, producing increased levels of air ingress. If the air leakage to the flue gas stream increases, the flue gas volume becomes diluted, introducing an increase in toxic gas emissions levels. These conditions are symptoms of excessive fouling of air heater element packs, which can only be rectified by either applying frequent high pressure washing or replacement of element packs. Both of these are costly activities, which can be avoided by applying the correct operating conditions and maintenance strategies. Through evaluating air heater performance, and finding critical parameters that create rotary regenerative air heater fouling conditions, a simulation model was developed to predict the onset of dew point related fouling.

The above conditions are symptoms of excessive fouling of air heater element packs, which require frequent high pressure washing or replacement of element packs. Dew point related fouling exists when the flue gas temperature and surrounding materials experience a temperature below the flue gas dew point temperatures. The fly ash particles in the flue gas adhere to each other and element pack surfaces when these conditions occur. Sulphuric acid, sulphurous acid, and moisture in the flue gas produce dew point related fouling. When precipitation inside the small spaces between the elements occur, the packs experience excessive clogging of ash deposits [3]. This process reduces the flow passages through the element packs. During normal operation, continuous exposure to high temperatures and drying (from the conditions internal to the air heater) cures and hardens the deposits between the elements. If the soot blowing system cannot remove the deposits, complete blocking of element packs will be the result. The application of correct operating conditions and maintenance strategies will mitigate the risk of incurring these costly activities. This research aimed to evaluate air heater performance through identification of critical parameters causing rotary regenerative air heater fouling conditions. These parameters were used to develop a simulation model to predict the onset of dew point related fouling. The research included plant experiments to validate the model.

2 Literature Overview

2.1 Regenerative Air heater Model

Caby and Gruen used a physical model to define correlations used to evaluate the heat transfer and pressure drop correlations of a thermal test facility used for developmental research of a regenerative air heater model [4, 5]. These correlations were later used by Habbitts to develop a mathematical model for rotary regenerative air heaters, known as the RAH model. A finite difference technique, to analyse the heat transfer for transient tests, by Mullison and Loerhke, was used by Caby and Habbitts to calculate the performance characteristics of the air heaters [6, 7]. This model was further developed by De Klerk, to estimate the fluid temperatures, element surface metal temperatures and differential pressure across the steel matrix for alternating thicknesses of element plates [8]. The following assumptions were made by Habbitts, and later reviewed by De Klerk, which was also considered during this research project [9]:

- Steady flow conditions are experienced flowing into and out of the air heater.
- The width and number of plates are sufficient to essentially reduce the problem to a one dimensional setup, with one directional flow in each block.
- Finite thermal conduction occurs in the solid parallel to the direction of flow, with no transverse temperature gradients. Thus the boundary conditions for the side walls of the elements are adiabatic. (As indicated in Figure 2 from section 4, below along the top and bottom plate centre lines.)
- Convection heat transfer occurs across the solid surface interfaces within the element. The magnitude of which is determined by a heat transfer coefficient h (temperature dependant). A single h value is assumed to apply throughout a particular block of plates at a particular instant in time. This is a space averaged convective heat transfer coefficient assumed to be applied across a series of parallel plates for a particular flow rate.
- All plates are made from the same material.
- The fluid thermal capacity is negligible in comparison with the solid thermal capacity.
- The effect of heat transfer by radiation is neglected due to its small contribution to the temperature difference between plate regions. The symmetrical gas molecules do not

participate in radiation, and the concentration of water vapour in air is too small. Therefore radiation from the air stream can be neglected. Radiation from the flue gas to the plates can be significant owing to temperatures differences of up to 40°C between gas and the plates. This effect is ignored due to the temperature difference occurring over small regions at the hot end of the matrix. Once a temperature drop is experienced, the effect of radiation decreases rapidly.

- The fluid flowing into and out of the control volume is considered to be at a steady state. This assumption is used for the formulation of the energy balance of the volume in Figure 2 in section 4. The energy exchanges across the boundaries of each region are assumed to be represented by conduction in the solid parallel to the direction of flow (this effect is also known as longitudinal conduction), convection between the solid and fluid region, and enthalpy flux into and out of the fluid region. Energy is stored within the solid regions and is proportional to thermal capacity of the solid.
- The mass flowrate for each block of plates for specific fluid stream is constant, but the temperature along with densities and velocities do change with time.

2.2 Dew point related fouling

Mathebula used a Quantitative Evaluation of Minerals by Scanning Electron Microscopy (QEMSCAN) surficial and cross-sectional analysis, to show the phases of fouling of ash deposits from an Eskom Power Station. These phases were anhydrite, AlSi-sulphate, Si (Al)-sulphate, iron sulphate and sulphur. The phases occur because of a reaction between sulphuric acid and fly ash components, and a reaction between sulphuric acid and fuel oil catalysts [10]. Kunze proposed the acid dew point concept based on the gas-liquid equilibrium. Therefore, the acid dew point was defined as the temperature of gas-liquid equilibrium interface when the apparent partial pressures of sulphuric acid vapour and water vapour at the interface equal to those in the flue gas [Kunze]. Sulphuric acid dew point temperatures vary according to changes in partial pressure for moisture (H₂O) and sulphur-trioxide (SO₃). Mathebula also concluded that fly ash adhere to the sulphuric acid that condenses onto the air heater plates, along with the fly ash particles adhering to each other when the gas temperature reduces below the sulphuric acid dew point temperature. The formation from the phases also shows that the sulphuric acid reacts with fly ash components and fuel oil char [10].

Wei compared the experimental data from previous acid dew point prediction methods using empirical formulas and the iterative calculation model. This comparison showed small deviations between the calculation results and experimental results, except for the studies of Haase & Borgmann and experimental constants-1 method. The results of Haase & Borgmann were abnormally low, while the results of experimental constants-1 showed a large-span increase, and the greatest deviation was around 41 °C [12]. Müller ignored the influence of water vapour on acid dew point, which resulted in under estimation of acid dew point temperatures. Halstead took the content of water vapour into consideration, but the results did not concur with the experiment data. The predictions of Verhoff & Branchero agreed well with the experimental data, and was found to be the preferred option. Verhoff & Branchero were the lowest compared with other deviations between other formula results and experimental data. Therefore, the prediction of Verhoff & Branchero is of great accuracy and has a wide range of application [12]. Ganapathy and Mathebula used Verhoff & Branchero's equation to calculate dew point temperatures (water, sulphuric acid and sulphurous acid) of flue gas [12, 11, 10].

3 Project Definition

The aim of the project was to develop a rotary regenerative air heater simulation model to predict the onset of dew point related fouling. This model aims to equip system engineers with the knowledge to enhance operating conditions and maintenance strategies, in order to prevent the onset of dew point related fouling. The study contributes to the possibility of increasing the life expectancy of air heater element packs and draught group components. It also contributes to improved boiler efficiency, reduced maintenance costs and production losses, which will conduce to improved and sustainable operating of coal fired power generation plants. The current maintenance approach incorporates a more reactive approach, and therefore creating preventative maintenance measures will be beneficial to Eskom. The following objectives were set in place to establish whether steel matrix metal temperatures can be controlled to prevent dew point related regenerative air heater fouling:

1. Identified dew point related fouling parameters.
2. Developed a modelling tool that predicts dew point operating conditions in a rotary regenerative air heater (VBA RAH model).
3. Verified the fouling condition by plant experiments to prove the accuracy of the VBA RAH model. The plant experiments comprised:
 - a. Measurements of fluid (Air and flue gas) temperatures for each layer of the steel matrix.
 - b. Measurements of metal surface temperatures for each layer of the steel matrix.
 - c. Air heater leakage and operating parameters.
 - d. Coal analysis which established coal composition.
 - e. Flue gas analysis which established flue gas composition.

4 Theoretical Analysis

4.1 Regenerative air heater simulation model theory

For this research project the following theoretical basis was used to develop a rotary regenerative air heater model (Visual Basic for Application Regenerative Air Heater – VBA RAH) which incorporated a prediction of the onset of dew point related fouling. Figure 2 expresses the enhanced model for energy balance for the fluid region. This model forms the basis for estimating the temperature profiles of both the fluid and the solid regions. Equation 4.1 illustrates the effect of the occurrence of convection, where equation 4.2 and 4.3 consider the solid regions where conduction occurs because of the convective effect of the fluid region [8].

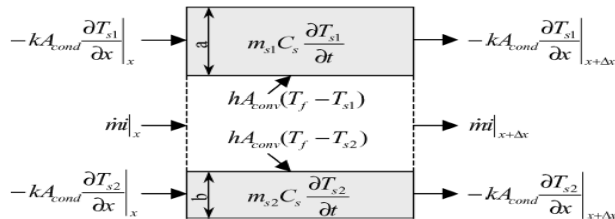


Fig. 2. Basic plate/channel element [9].

Fluid region:

$$\frac{\partial T_f}{\partial x} + \frac{h \cdot W}{\dot{m}_{fluid} C_f} (2T_f - T_{s1} - T_{s2}) = 0 \quad (4.1)$$

Each solid region temperature profile will be formulated using:

Solid 1:

$$\frac{\partial T_{s1}}{\partial t} = \frac{k}{\rho_s C_s} \frac{\partial^2 T_{s1}}{\partial x^2} + \frac{h}{\rho_s C_s a} (T_f - T_{s1}) \quad (4.2)$$

Solid 2:

$$\frac{\partial T_{s2}}{\partial t} = \frac{k}{\rho_s C_s} \frac{\partial^2 T_{s2}}{\partial x^2} + \frac{h}{\rho_s C_s a} (T_f - T_{s2}) \quad (4.3)$$

Dimensionless parameters are used as part of the numerical method. T^* is the dimensionless temperature and can be calculated using the following equation:

$$\frac{\partial T_{s2}}{\partial t} = \frac{k}{\rho_s C_s} \frac{\partial^2 T_{s2}}{\partial x^2} + \frac{h}{\rho_s C_s a} (T_f - T_{s2}) \quad (4.4)$$

The following equations are used to convert the heat transfer parameters to non-dimensional parameters:

1. Dimensionless time:

$$\theta = \frac{\dot{m} C_f}{M_s C_s} \quad (4.5)$$

2. Conduction Parameter:

$$\lambda = \frac{k A_{cond}}{\dot{m} C_f L} \quad (4.6)$$

3. Dimensionless length:

$$z = \frac{x}{L} \quad (4.7)$$

4. Number of transfer units:

$$NTU = \frac{h A_{conv}}{\dot{m} C_f} \quad (4.8)$$

5. Thickness Ratio:

$$\beta = \frac{a}{b} \quad (4.9)$$

Dimensionless temperatures must be calculated for both solid regions and the fluid region:

$$T_f^* = (T_f - T_{cold\ inlet}) / (T_{hot\ inlet} - T_{cold\ inlet}) \quad (4.10)$$

$$T_{s1}^* = (T_{s1} - T_{cold\ inlet}) / (T_{hot\ inlet} - T_{cold\ inlet}) \quad (4.11)$$

$$T_{s2}^* = (T_{s2} - T_{cold\ inlet}) / (T_{hot\ inlet} - T_{cold\ inlet}) \quad (4.12)$$

Therefore rewriting the equation 4.1 to 4.3 by substituting in the non-dimensional parameters:

Fluid region:

$$\frac{\partial T_f^*}{\partial z} + NTU \left(T_f^* - \frac{T_{s1}^* + T_{s2}^*}{2} \right) = 0 \quad (4.13)$$

Solid 1:

$$\frac{\partial T_{s1}^*}{\partial \theta} = \lambda \frac{\partial^2 T_{s1}^*}{\partial z^2} + \frac{NTU}{2} \left(1 + \frac{1}{\beta} \right) (T_f^* - T_{s1}^*) \quad (4.14)$$

Solid 2:

$$\frac{\partial T_{s2}^*}{\partial \theta} = \lambda \frac{\partial^2 T_{s2}^*}{\partial z^2} + \frac{NTU}{2} (1 + \beta) (T_f^* - T_{s2}^*) \quad (4.15)$$

The same assumptions from the research conducted by Habbitts and De Klerk mentioned in section 2.1 were used [9]. The solution for the above mentioned equation uses the standard difference approximations and Crank- Nicholson implicit method. These three equations (equations 4.13 to 4.15) provide a method to calculate the temperatures for both solid regions and the fluid region along the elements at any point in time. Figure 3 is an illustration of the finite difference elements. A system of equations can now be planned in a matrix form. The non-dimensional parameters are substituted into equation 4.13 to 4.15, and then used in a finite difference scheme illustrated in equations 4.16 to 4.22:

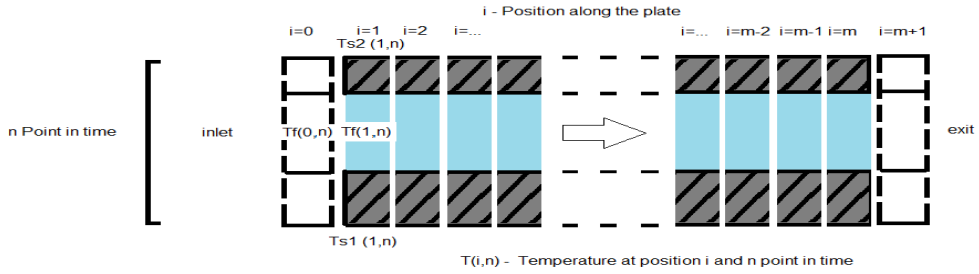


Fig. 3. Discretization of a flat double plated region into finite difference elements.

Fluid region:

$$\frac{T_f^*(i,n) - T_f^*(i,n)}{\Delta z} + NTU \left(T_f^*(i,n) - \frac{T_{s1}^*(i,n) - T_{s2}^*(i,n)}{2} \right) = 0 \quad (4.16)$$

Solid 1:

$$\frac{T_{s1}^*(i,n+1) - T_{s1}^*(i,n)}{\Delta \theta} = \lambda(X + Y) + \frac{NTU}{2} \left(1 + \frac{1}{\beta} \right) \left(T_f^*(i,n) - T_{s1}^*(i,n) \right) \quad (4.17)$$

Solid 2:

$$\frac{T_{s2}^*(i,n+1) - T_{s2}^*(i,n)}{\Delta \theta} = \lambda(X + Y) + \frac{NTU}{2} \left(1 + \frac{1}{\beta} \right) \left(T_f^*(i,n) - T_{s2}^*(i,n) \right) \quad (4.18)$$

X and Y can be substituted with:

Solid 1:

$$X = \frac{T_{s1}^*(i+1,n+1) - 2T_{s1}^*(i,n+1) + T_{s1}^*(i-1,n+1)}{2\Delta z^2} \quad (4.19)$$

$$Y = \frac{T_{s1}^*(i+1,n) - 2T_{s1}^*(i,n) + T_{s1}^*(i-1,n)}{2\Delta z^2} \quad (4.20)$$

Solid 2:

$$X = \frac{T_{s2}^*(i+1,n+1) - 2T_{s2}^*(i,n+1) + T_{s2}^*(i-1,n+1)}{2\Delta z^2} \quad (4.21)$$

$$Y = \frac{T_{s2}^*(i+1,n) - 2T_{s2}^*(i,n) + T_{s2}^*(i-1,n)}{2\Delta z^2} \quad (4.22)$$

The above mentioned equations are numerically solved to find the metal surface temperature along with the fluid temperature profiles for a rotary regenerative air heater.

4.2 Dew point related fouling theory

Sulphurous- and sulphuric acid formation occurs during condensation of water vapour in the flue gas. This further reacts with the ash alkaline elements, resulting in air heater fouling. The dew point temperature is therefore one of the critical parameters requiring governance to operate above of the metal temperature. This process will avoid sulphuric acid deposition. The three critical dew point temperatures to be taken into consideration are the dew point temperature of water vapour, sulphurous acid and sulphuric acid. Equation 4.23 is used to calculate the partial pressure P_i of the flue gas constituents [10]. The partial pressure for sulphur trioxide considers the percentage conversion initially assumed for the formation of sulphur trioxide (ranges from 1% to 5% of SO_2 to SO_3).

$$P_i = \left(\frac{\% \text{ mole fraction}}{100} \right) \times P \quad (4.23)$$

The partial pressure for water vapour and steams tables are used to find the dew point temperature of water vapour.

$$P_{H_2O} = \left(\frac{\%H_2O}{100}\right) \times P \quad (4.24) ; \text{ Find } T_{H_2O} \text{ from the steam tables}$$

The sulphurous acid dew point temperature estimation uses the partial pressures for water vapour and sulphur dioxide in equation 4.26 and 4.27 for the variable a, and b in equation 4.25 [11, 12].

$$\frac{1000}{T_{dp}} = 3.9526 - (0.1863 \times a) + (0.000867 \times B) - (0.000913 \times a \times b) \quad (4.25)$$

$$a = \ln(P_{H_2O}) \quad (4.26)$$

$$b = \ln(P_{SO_2}) \quad (4.27)$$

The sulphuric acid dew point temperature estimation uses the partial pressures for water vapour and sulphur trioxide as shown in equation 4.29 and 4.30 for the variable c, and d in equation 4.28.

$$\frac{1000}{T_{dp}} = 2.276 - (0.0294 \times c) - (0.0858 \times d) + (0.0062 \times c \times d) \quad (4.28)$$

$$c = \ln(P_{H_2O}) \quad (4.29)$$

$$d = \ln(P_{SO_3}) \quad (4.30)$$

5. Results

5.1 Sulphuric acid dew point temperature ranges

Figure 4 is an illustration of the sulphuric acid dew point temperatures for the three conditions of testing. From these results it is clear that the cold end layer mostly operate in the critical temperature ranges. With insufficient soot blowing the deposits harden and cause excessive fouling of air heaters. Sulphurous acid and moisture dew point temperatures are not reached during normal operation, only during a light up or shut down of a unit.

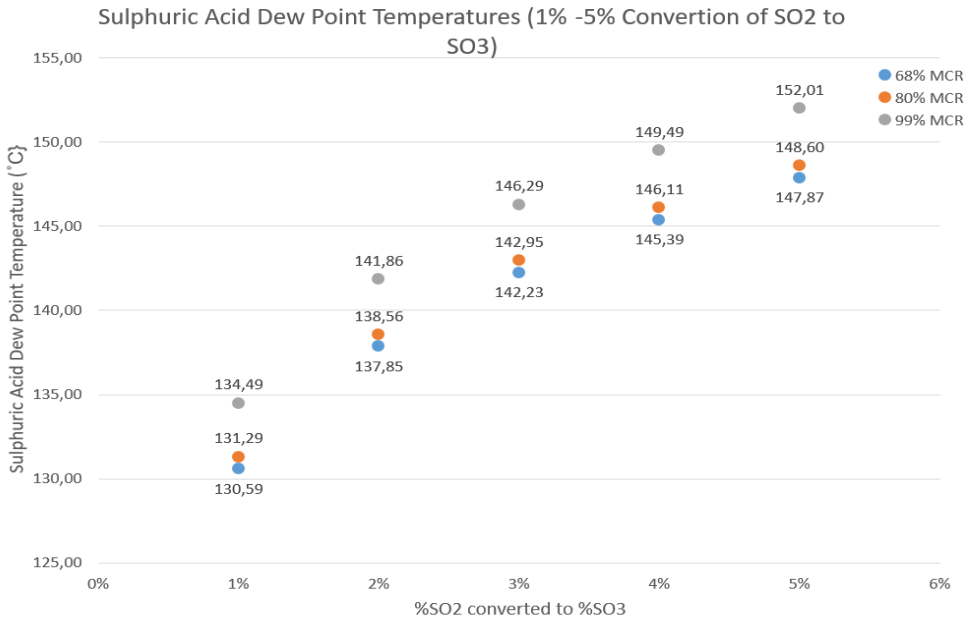


Fig. 4. Sulphuric acid dew point temperatures for 1% to 5% SO₂ to SO₃ conversion

This test considered three different load conditions (68%MCR - Maximum Continuous Rating, 80%MCR and 99%MCR). Measurement of the inlet and outlet metal- and fluid (Flue gas and air) temperatures for each layer of element packs, along with air heater leakage, were taken. The test also considered coal composition and flue gas compositions measured by an Eskom Research Testing & Development team. This measurement included SO₂% (volumetric) and moisture to estimate the relevant dew point temperatures. Coal composition provided input parameters to a mass balance for products of combustion. This allowed validation of the measured flue gas composition. A 1% to 5% range of SO₂ to SO₃ conversion were used for all three cases. The following results were obtained:

99% MCR: For 1% - 5% conversion of SO₂ to SO₃, 90% - 100% of the simulated metal temperatures at the cold end layer were exposed to sulphuric acid dew point conditions (25 seconds of the total 27 seconds of flue gas exposure). The measured metal temperatures were exposed completely (As shown in Figure 5).

80% MCR: For 1% - 5% conversion of SO₂ to SO₃, 81% - 100% of the simulated metal temperatures at the cold end layer were exposed to sulphuric acid dew point conditions (22 seconds of the total 27 seconds of flue gas exposure). The measured metal temperatures were exposed completely.

68% MCR: For 1% - 5% conversion of SO₂ to SO₃, 37% - 100% of the simulated metal temperatures at the cold end layer were exposed to sulphuric acid dew point conditions (10 seconds of the total 27 seconds of flue gas exposure). The measured metal temperatures experienced 46% - 100% exposure.

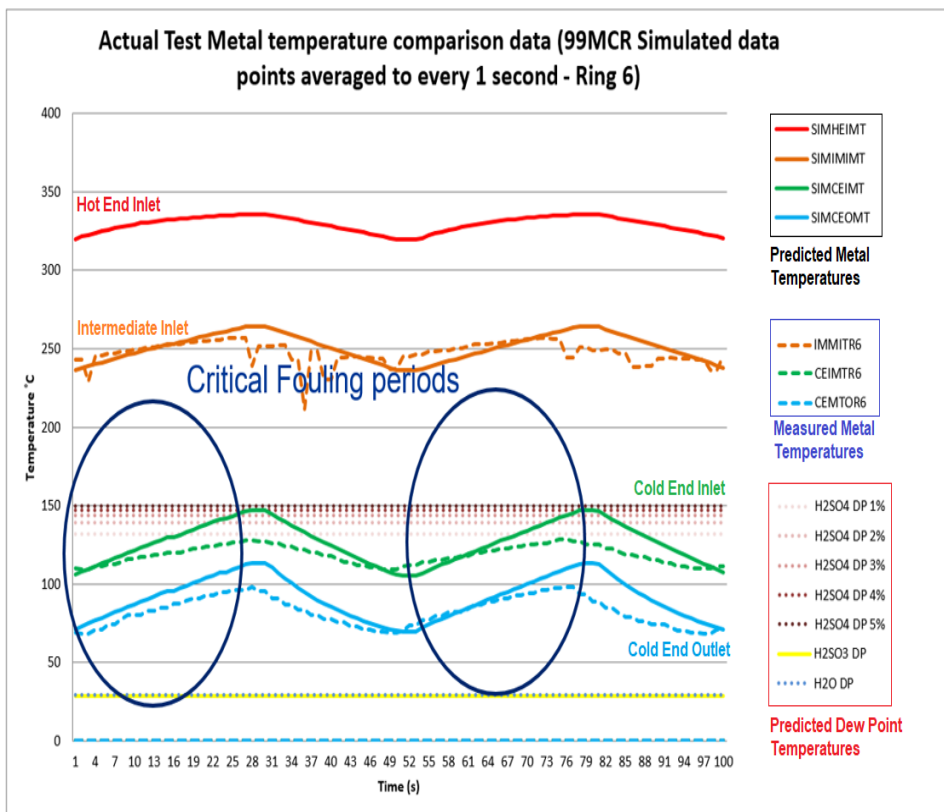


Fig. 5. Operating metal temperature for one full rotation per layer. (Simulated temperatures versus measured temperatures at 99%MCR)

Further validation of the VBA RAH model was done by comparing results from research conducted by Habbitts (1998) and De Klerk (2001). The major contributor to errors in this research, related to the omission of a K factor for the 99%MCR condition velocity measurement calculations. A factors of 0.85 were included which improved the correlations between the experimental and theoretical results. The RAH (De Klerk, 2001) model and recently developed VBA RAH model showed good correlation. This validation process proved that the VBA RAH model can be used as a tool to identify methods to optimize air heater performance. Figure 6 is an illustration of the correlation between the measured values from the research conducted by Habbitts and the simulation results for the RAH and the VBA RAH model.

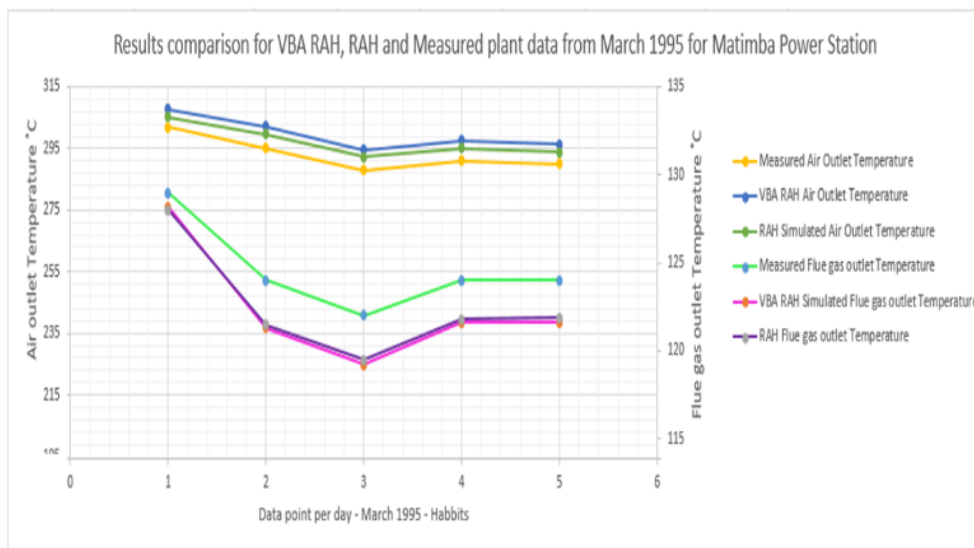


Fig. 6. Result comparison for the VBA RAH, RAH and measured plant data from tests conducted in March 1995 at Matimba Power Station.

Comparing the measured values to the simulated values, the correlation was fair but still not ideal, and some form of error existed. It was a challenging environment to measure temperate because of high levels of ash in the flue gas, and the element pack configuration in the steel matrix. Unaccounted for thermal inertia (affected by ash and wear protection), contact resistance, ash accumulation in perforated areas and incorrect flue gas flow measurements contributed to this error. An average deviation of 7.29% were found for the three load conditions. For the comparison of measured and simulated data, the 68% MCR condition showed the best correlations. The largest deviation existed for the 99% MCR condition, which was caused by an omission of a K factor during velocity measurements. The flow kinetics manometer used has a specified K factor of 0.85. This factor was included and the correlation between measured and simulated data improved, and the average deviation for the three loads reduced to 2.17%. Because of non-ideal allocation of measuring ports, the K factor was further reduced to 0.80 to find an ideal flow rate to match for the 99% MCR measured operating parameters. The average deviation between loads reduced to a 4.23% after this change, which proved that the 0.85 K factor is the preferred option.

The model also provides the ability to amend operating parameters to estimate changes in boiler performance. The inlet temperature was raised to 70 degrees which resulted in a 1.6 MW reduction in energy input to the boiler. The coal flow reduced by 0.1 kg/s and the boiler efficiency improved by 0.2%. The cost saving with regards to a reduction in coal flow is R1

127 033.57 per year. Changing the operating conditions in this way can be used as a method to reduce dew point related fouling, but this option is limited by the capacity of the pre-steam air heater and the fan design temperature. For the FD fans, the design maximum temperature is 50°C. If the air temperature is increased beyond this point the fan will operate with air densities outside of its design range. Due to the fact that the fan is a constant volume machine, the volumetric flow rate will be maintained. With this in mind the density will decrease with an increase in temperature. This process reduces the pressure difference across the fan, but requires increased radial vane positions to maintain the required operating pressure after the air heaters. Other options were evaluated and the option of increasing the air temperature to 50°C and removal of the third layer of element packs showed promising results. This estimated a reduction in the onset of dew point related fouling, and improving the boiler performance. Therefore this was a recommendation for further research with experimental validation.

6. Conclusion

The VBA RAH model was successfully developed to predict the onset of dew point related fouling and provides a platform to equip system engineers with the knowledge to enhance air heater performance. The research showed that the VBA RAH model can help improve life expectancy of air heater element packs and draught group components such as ducting, dampers and supply joints. It also proves to reduce the risk of the occurrence of dew point related fouling, and improve cleaning capacity of the element packs. Air heater operating and design amendments were simulated to evaluate the impact on overall boiler performance. The following solutions to reduce dew point related fouling were suggested:

1. Increasing the air inlet temperatures from 35°C to 70°C.
2. Removing the third layer of element packs.
3. Removing the third layer and increase the air inlet temperatures to 50 °C.

The third option is a promising solution to reduce the onset of dew point related fouling and is recommended for further research through plant experiments. Although the simulation results did not show ideal correlations to the measured performance at all times, the impact assessment of boiler performance because of changes in air heater design and operating parameters proves to be valuable. This platform provides methods to improve boiler efficiency, reduce maintenance costs and production losses, which will conduce to improved and sustainable operating of Eskom coal fired power generation plants.

Nomenclature

\dot{m} – Mass flow of fluid
 C_f – Heat capacity of the fluid
 M_s – Mass of the solid material of the element pack
 C_s – Heat capacity of the solid material of the element pack
 k – Conductivity of the solid material of the element pack
 L – Length element pack (height of the element pack)
 x – Length of the pack at the given time interval
 a – Half of the thickness of the corrugated solid region
 b – Half of the thickness of the undulated solid region
 A_{conv} – Area of convection at the given time interval
 A_{cond} – Area of conduction at the given time interval
 h – Average heat transfer coefficient
 T_f - Fluid temperature

T_{s1} - Corrugated solid temperature
 T_{s2} - Undulated solid temperature
 T_f^* - Dimensionless fluid temperature
 T_{s1}^* - Dimensionless corrugated solid temperature
 T_{s2}^* - Dimensionless undulated solid temperature

References

1. H. Kleynhans, J. Eganza, ID Fans at Maximum Capacity. Guideline-Possible Causes and Contributors Guideline, ESKOM Technology Engineering Guidelines, Johannesburg (2016).
2. W. Brandt, Unit 2 BMFT due to inadequate secondary air flow (<20% BMCR), ESKOM Matimba Power Station, South Africa, Lephallale (2015).
3. W. Brandt, Engineering Change Root Cause Analysis for Air heater Ash fouling Report, Eskom Matimba Power Station Engineering ECM –RCA documentation, South Africa, Lephallale (2018).
4. K. Gruen, Heat transfer and pressure drop of regenerative air pre-heaters elements, MSc (Eng.) dissertation, University of the Witwatersrand, Johannesburg (1998).
5. M. J. Caby, Experimental Investigation of Heat Transfer in Regenerative Heat Exchangers, MSc (Eng.) dissertation, University of the Witwatersrand, Johannesburg (1996).
6. S. Habbitts, “Computer Simulation of Power Station Regenerative heat exchangers,” MSc (Eng.) dissertation, University of the Witwatersrand, Johannesburg (1998).
7. R. I. Loehrke R. S. Mullisen, A transient heat exchanger evaluation test for arbitrary fluid inlet temperature variation and longitudinal core conduction, J. of H. T., 108, May 1986.
8. G. De Klerk, An Improved Simulation Model for Rotary Regenerative Air Heaters,” MSc (Eng.) dissertation, University of the Witwatersrand, Johannesburg (2001).
9. G. B. De Klerk, T. J. Sheer, H. H. Jawurek, M Lander., A Versatile Computer Simulation Model for Rotary Regenerative Heat Exchangers, H. T. Eng., 1-13, 3 April (2013).
10. N. V. Mathebula, Observation and the classification of the fouling mechanisms in rotary air heaters, MSc (Eng.) dissertation, University of the Witwatersrand, Johannesburg (2014).
11. V. Ganapathy, Cold end corrosion: Causes and cures, Abeline: ABCO Ind., 57-59, USA, Texas (1989).
12. W. Wei, Theoretical prediction of acid dew point and safe operating temperature of heat exchangers for coal-fired power plants, Apl. Therm. Eng., 782-790, 123 (2017)